

# “Annular Ring” microtubes formed by SDS@2 $\beta$ -CD complexes in aqueous solution†

Lingxiang Jiang,<sup>a</sup> Yu Peng,<sup>a</sup> Yun Yan,<sup>a</sup> Manli Deng,<sup>b</sup> Yilin Wang<sup>b</sup> and Jianbin Huang<sup>\*a</sup>

Received 2nd October 2009, Accepted 18th January 2010

First published as an Advance Article on the web 3rd March 2010

DOI: 10.1039/b920608f

Traditional aqueous self-assembly of tubular structures (as well as other aggregates) usually relies on the hydrophobic effect, a relatively weak and nondirectional interaction. The resultant aggregates are inherently soft, fluid, and less-ordered. Alternatively, we report a novel kind of nonamphiphilic self-assembly of microtubes in aqueous solutions of cyclodextrin/ionic surfactant (CD/IS) complexes. This self-assembly is driven exclusively by H-bonds, relatively strong, directional interactions. The CD/IS microtubes feature an unbundling nature, ultralong persistence lengths, highly monodispersed diameters, and remarkable rigidity. Every single CD/IS microtube is constituted by a set of coaxial, equally spaced, hollow cylinders, resembling the annular rings of trees (thus termed as “annular ring” microtubes). Furthermore, bearing in mind the fundamental difference between the amphiphilic counterpart in driving forces, this H-bond-driven hydrophilic self-assembly is envisioned to complement its counterpart and expand the field of molecular self-assembly.

## Introduction

Molecular self-assembly, a ubiquitous process in chemistry, materials science, and biology, provides a path towards ordered, functional structures including micelles, vesicles, helices, and tubes.<sup>1</sup> Among them, tubular structures<sup>2</sup> have received increasing attention because of their fruitful applications in device fabrication, templated synthesis, drug release, and biosensing, to name a few.<sup>3</sup> Extensive efforts were thus exerted to identify the architectures of tube-forming molecules, which by now have covered a wide variety of molecules such as lipids, bola-amphiphiles, peptides, and aromatic amphiphiles.<sup>2,3</sup> It is worth noting that most of these building blocks are of an amphiphilic nature and their assembly into tubes is mainly driven by the hydrophobic effect (the tendency of hydrophobic moieties to aggregate to minimize contact with water).<sup>4</sup> The hydrophobic effect, however, appears to be relatively weak and nondirectional; the resultant tubes are inherently soft and fluid.<sup>4</sup> Alternatively, the hydrogen bond (H-bond), a relatively strong, directional, and recognizable interaction, could be an ideal candidate to replace the hydrophobic effect. Despite their potential advantages, H-bonds have scarcely been employed as the driving force for the aqueous self-assembly of tubes (as well as other aggregates) in the absence of the hydrophobic effect.<sup>5</sup> In addition, the practical aspects of the tubes (*e.g.*, length, rigidity, and monodispersity) are critical to their applications. It is therefore desirable to construct long, rigid, and monodispersed tubular structures. Herein, we report that the fully hydrophilic cyclodextrin/ionic surfactant (CD/IS) complexes are able to assemble in water into

well-defined microtubes, exclusively driven by H-bonding and mediated by electrostatic interactions (Fig. 1). The CD/IS microtubes feature an unbundling nature, ultralong persistence lengths, highly monodispersed diameters, and remarkable rigidity. Furthermore, every single CD/IS microtube is constituted by a set of coaxial, equally spaced, hollow cylinders, resembling the annular rings of trees (thus termed as “annular ring” microtubes).

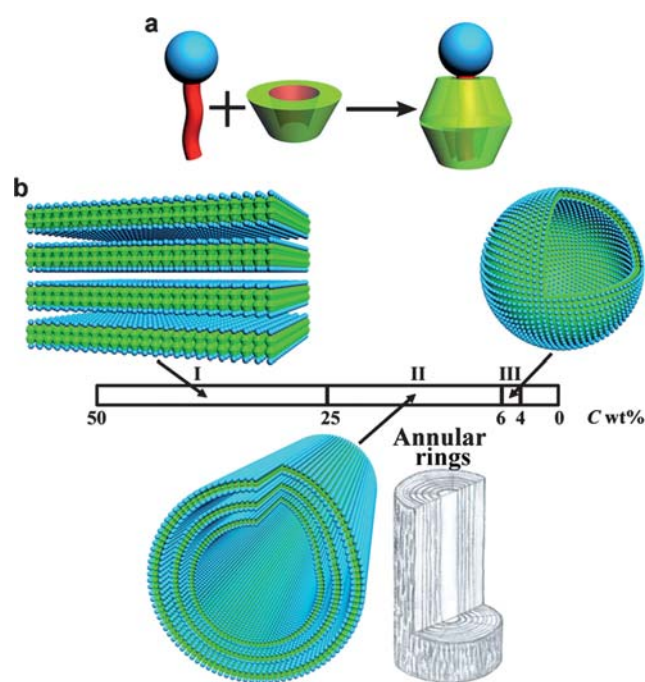


**Fig. 1** A schematic of the self-assembly behavior of SDS@2 $\beta$ -CD, with the coaxial, equally spaced, hollow cylinders, resembling annular rings.

<sup>a</sup>Beijing National Laboratory for Molecular Sciences (BNLMS), State Key Laboratory for Structural Chemistry of Unstable and Stable Species, College of Chemistry and Molecular Engineering, Peking University, Beijing 100871, P. R. China. E-mail: jbhuan@pku.edu.cn

<sup>b</sup>Institute of Chemistry, Chinese Academy of Sciences, Beijing, China

† Electronic supplementary information (ESI) available: A CLSM image, WAXS patterns and fluorescence spectra. See DOI: 10.1039/b920608f

We chose the CD/IS complexes as the building blocks of the H-bond-directed aqueous self-assembly due to the following considerations. CDs are donut-like oligosaccharides with a hydrophilic outer surface (with abundant H-bond sites) and hydrophobic cavities (capable of including a variety of guests).<sup>6</sup> The multiple H-bond sites serve to overcome the strong competitiveness from water and to drive the building blocks to aggregate. These sites, however, seem to provide excess attractions for assembly, as suggested by crystalline precipitation in many CD or CD/guest aqueous solutions.<sup>7</sup> To mediate the excessive attractions, electrostatic repulsions can be imposed by selecting ionic surfactants as the guests. The resulting CD/IS complexes are fully hydrophilic, and their CD bodies and ionic headgroups are expected to drive and mediate the self-assembly, respectively.

## Experimental section

All the reagents were purchased from commercial sources. For FF-TEM, samples were frozen by liquid propane; fracturing and replication were carried out in a freeze-fracture apparatus (BalzersBAF400, Germany) at  $-140\text{ }^{\circ}\text{C}$ ; Pt/C was deposited at an angle of  $45^{\circ}$  to shadow the replicas, and C was deposited at an angle of  $90^{\circ}$  to consolidate the replicas; the resulting replicas were examined in a JEM-100CX electron microscope. CLSM observations were carried out by a TCS-sp inverted microscope (Leica, Germany). AFM measurements were conducted by Nanoscope IIIa (Digital Instruments Inc., USA) in tapping mode under ambient conditions. SAXS and WAXS measurements were performed by SAXSess (Anton-Paar, Austria, Cu K $\alpha$ ,  $\lambda = 0.154\text{ nm}$ ), in which samples were sealed in quartz capillary tubes. Fluorescence spectra were recorded by a FLS 920 spectrometer (Edinburgh Instruments Ltd., UK).

## Results and discussion

### Preliminary phase behavior

As an exemplary system, we focused on aqueous mixtures of  $\beta$ -CD and sodium dodecyl sulfate (SDS, one of the most common anionic surfactant). In aqueous solution,  $\beta$ -CD can spontaneously form an inclusion complex with SDS in a 2 : 1 stoichiometry with a high binding constant,<sup>8</sup> in which one SDS aliphatic chain is embedded into two  $\beta$ -CD cavities and the complex is thus termed as “SDS@2 $\beta$ -CD”. For sample preparation, desired amounts of  $\beta$ -CD, SDS, and water were weighed into tubes to give a constant  $\beta$ -CD : SDS molar ratio of 2 : 1 and different total concentrations of  $\beta$ -CD and SDS ( $C$ , in wt%); the samples were heated to obtain transparent and isotropic solutions, where SDS@2 $\beta$ -CD is formed as the major composition; the solutions were then thermostatically incubated at  $25\text{ }^{\circ}\text{C}$  (for at least 48 h) to form SDS@2 $\beta$ -CD aggregates. The aggregates are considered to be spontaneously formed because no energy input (such as sonication or extrusion) is involved. The solutions and aggregates are stable for months, as verified by repeatable results after a long incubation time.

Along the concentration axis of  $C$ , three regions with different aggregates were identified (Fig. 1b). In region I ( $C = 50\text{--}25\text{ wt}\%$ ), the solutions are semi-transparent and display strong static birefringence under a crossed polarizer, indicative of an

anisotropic phase. This phase was found to be a pure lamellar phase. In region II ( $C = 25\text{--}6\text{ wt}\%$ ), the solutions are opalescent and viscoelastic, indicating the presence of aggregates that are both of large size to strongly scatter light and of high length-to-diameter ratios to enhance the viscoelasticity. This phase was found to be dominated by microtubes. In region III ( $C = 6\text{--}4\text{ wt}\%$ ), the solutions are of a bluish appearance and a water-like viscosity, both of which parallel those of typical lipid vesicular solutions. This phase was found to be dominated by vesicles. Here, we will focus on region II and the microtubes while the results of region I and III are prepared as a separate paper.

### “Annular ring” microtubes

For samples in region II, several mutual complementary microscopy techniques were employed to investigate the morphologies of the aggregates therein. Representative results of the  $C = 10\text{ wt}\%$  system are shown below. After staining by a trace amount of a fluorescent dye, Nile Red (NR), the samples were observed in a hydrated state by confocal laser scanning microscopy (CLSM) in fluorescence mode. It was reported that NR can be partly inserted into  $\beta$ -CD cavities in  $\beta$ -CD aqueous solution,<sup>9</sup> NR is thus anticipated to positively stain the aggregates in this case. In Fig. 2a and 2d, there are exclusively pairs of red fluorescent parallel lines separated by a non-fluorescent center, consistent with the longitudinal-sectional view of hollow tubular structures with their walls being positively stained. These uniform tubes pervade all over the images, exhibit diameters  $\sim 1\text{ }\mu\text{m}$  (thus termed as microtubes) and a mean length  $\sim 40\text{ }\mu\text{m}$ , and are open-ended (marked by big arrows in Fig. 2a). Similar elongated tubular structures are observed for the samples by CLSM in differential interference contrast (DIC) mode (Fig. 2b, not stained by NR) and transmission electron microscopy (TEM, Fig. 2c, not stained by heavy metals), which rules out the possibility that the added trace amount of NR will affect the microtubes.

After establishing the preliminary structure for the microtubes, we proceeded to identify their characteristics and structural details. First, the microtubes display features related to discreteness, length, monodispersity, and rigidity. As shown in Fig. 2a and 2d, although the microtubes are highly concentrated, they remain as isolated, unbundled entities with a wall-to-wall distance of  $\sim 0.7\text{ }\mu\text{m}$  for two neighboring tubes. Such well-defined separation suggests the existence of long-range repulsions (probably electrostatic repulsions) between the microtubes. The mean length ( $40\text{ }\mu\text{m}$ ) seems to be underestimated because the crowded environment will suppress microtube growth and the microtubes may be broken off into short ones under macroscopic shear during sample preparation (see Fig. S1 in the ESI†). Even so, there is still an appreciable amount of ultralong ( $\sim 100\text{ }\mu\text{m}$ ) microtubes, where two such microtubes crossing the whole image in the dotted region of Fig. 2d are highlighted in cyan. It is thus inferred that the persistence length of the microtubes is of the submillimeter order. Fig. 2e shows the statistical distribution of the tube diameters as collected from fluorescence images. The Gauss fitting therein manifests a highly monodispersed distribution (standard derivation  $\sigma = 0.05$  and mean diameter =  $1.1\text{ }\mu\text{m}$ ). Furthermore, the microtubes are of notable stiffness according to the two facts: (1) they are quite straight without

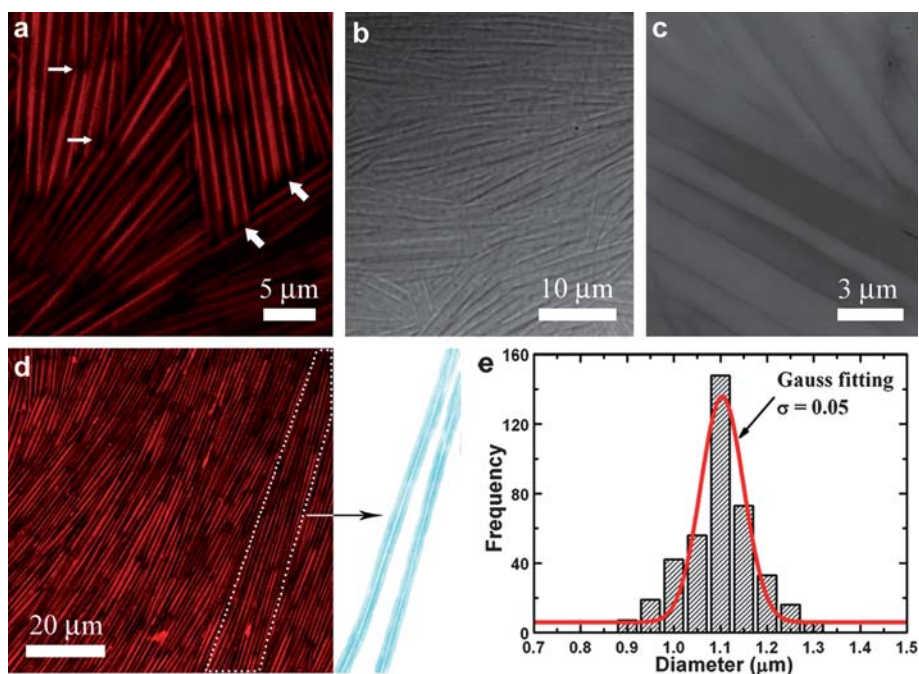


**Fig. 2** Morphologic investigations of the microtubes in the 10 wt% SDS@2 $\beta$ -CD solution. The images were acquired by CLSM in fluorescence (a, d) and DIC (b) modes, and by TEM (c). A histogram of the diameter distribution of the microtubes (e).

curving or bending even for the ultralong ones, and (2) when they cannot maintain straightness due to space limitation, they snap rather than bend (denoted by small arrows in Fig. 2a). In combination, the microtubes bear an unbundling nature, ultralong persistence lengths, highly monodispersed diameters, and distinctive rigidity.

Second, the present microtubes are multilamellar in nature and of a unique “annular ring” structure (*i.e.*, a set of coaxial, equally spaced, hollow cylinders). To unveil such a structure, we resorted to freeze-fracture transmission electron microscopy (FF-TEM)

that allows visualization of the inner architectures. In this technique, the samples were vitrified to preserve the structures and then fractured to expose cross sections of the structures; replicas of the fracture surface were shadowed by platinum and observed under TEM. In the present case, the microtubes are assumed to be randomly oriented in solution and the fracture surface will cross the microtubes at different angles. If  $\theta$  (the angle between the fracture surface and the radial plane of the “annular ring” microtubes) goes from  $0^\circ$  to  $90^\circ$ , one would expect the cross sections to be a set of concentric circles ( $\theta = 0^\circ$ ), a set of

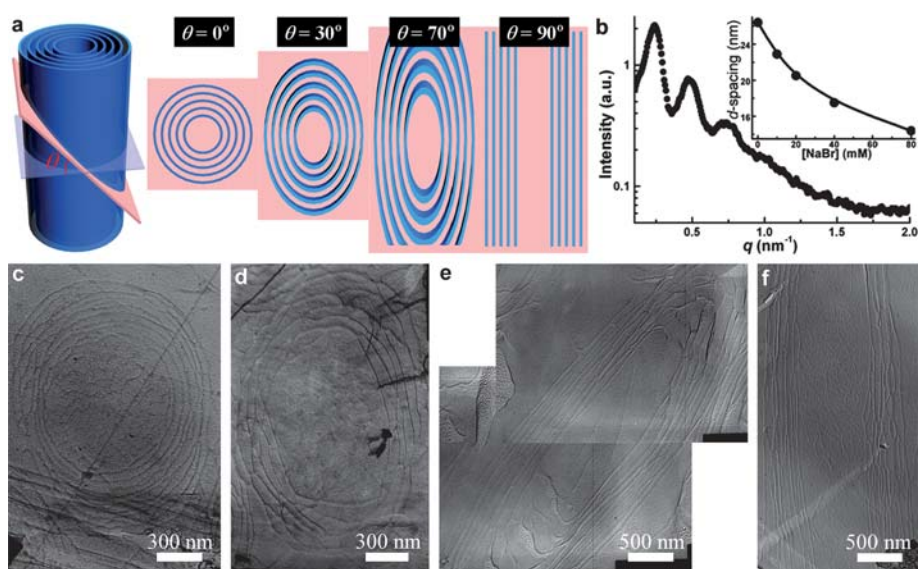


**Fig. 3** The “annular ring” structure of the microtubes. The cross sections of such a microtube with the increases of  $\theta$  (a). SAXS profile of the microtubes (b). The inserted figure shows the salt effect on  $d$ -spacing. FF-TEM micrographs of the microtubes with the fracture section at different angles (c–f), where  $\theta$  goes from 0 degrees to 90 degrees for (c) to (f).

concentric ellipses ( $0^\circ < \theta < 90^\circ$ ; the ellipses will gradually elongate upon increasing  $\theta$ ), and two sets of axisymmetrical parallel lines ( $\theta = 90^\circ$ ), as illustrated in Fig. 3a. The FF-TEM macrographs (Fig. 3c–3f) display circles, ellipses, elongated ellipses, and parallel lines exactly as expected, thereby confirming the “annular ring” structure. Meanwhile, the small-angle X-ray scattering (SAXS) profile of the sample (Fig. 3b) is characterized by Bragg peaks with regular spacing indexed as 1, 2, and 3, a typical pattern for lamellar structures. This result verifies that the hollow cylinders or tubular lamellae in a single microtube are coaxial and equally spaced. Moreover, the  $d$ -spacing from SAXS data as well as the FF-TEM observation reveal that two nearest tubular lamellae are well separated by a thick water layer. Therefore, this “annular ring” structure might enable the templated synthesis of multi-wall inorganic tubes in one step, which cannot be fulfilled by previous multilamellar lipid tubes with closely stacked lamellae. In addition, the  $d$ -spacing will be gradually decreased by adding excess NaBr (see the inserted plot in Fig. 3b), implying an electrostatic-stabilizing mechanism. It is worth noting that it is still not clear why and how the lamellae will fold into the annular ring tubes.

Third, the tubular lamellae are suggested to adopt a channel-type bilayer architecture in a molecular level according to atomic force microscopy (AFM) and wide-angle X-ray scattering (WAXS) results. In AFM analyses, samples were drop-coated on the freshly cleaved mica and the sample-loaded mica was examined in tapping mode. AFM measurements generally give relatively short, tape-like structures with far smaller heights than widths. These tapes are consistent with collapsed hollow microtubes, as supported by the coincidence of their perimeters. As shown in Fig. 4a and 4c, one of the collapsed microtubes happens

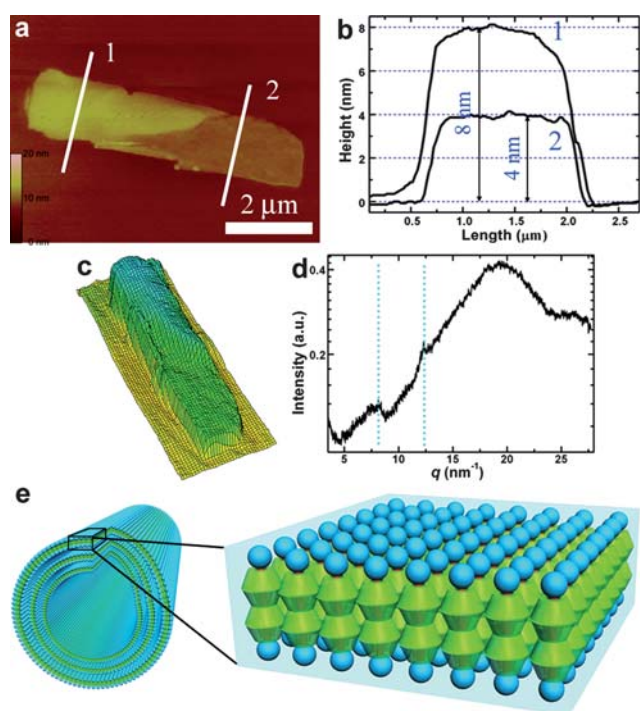


**Fig. 4** The structure of the tubular lamellae. An AFM height map (a), sectional analyses (b), and reconstructed 3-D height plot (c). The WAXS profile (d). A scheme of the proposed channel-type bilayer structure (e).

to be a unilamellar microtube with a part of its wall on one side being somehow peeled off. Its heights ( $\sim 8$  and  $4$  nm for the left and right parts, respectively, Fig. 4b) infer that the tubular lamellae are of a thickness ( $\sim 4$  nm) identical to double the length of SDS@ $2\beta$ -CD ( $\sim 2$  nm, by molecular modeling). This coincidence signals a bilayer structure without significant tilting or interpenetration. In the WAXS pattern in Fig. 4d, two diffraction peaks at  $8.2$  and  $12.4$  nm $^{-1}$  are recognizable (although quite weak), in line with the channel-type structure<sup>10</sup> of  $\beta$ -CD/guest complexes (for details, see the ESI<sup>†</sup>). For channel-type compounds,  $\beta$ -CD molecules will be aligned in a head-to-head fashion along the “channels” to maximize formation of H-bonds.<sup>10</sup> In light of the above results, we propose a channel-type bilayer architecture for the SDS@ $2\beta$ -CD tubular lamellae, as illustrated in Fig. 4e. Also, this architecture, with the ionic headgroups residing on the surface of each lamella, explains the two observations mentioned above, namely, the long-range repulsions between microtubes and electrostatically stabilized lamellae in each microtube.

### Discussion on the possible driving forces

There are three interactions, including the hydrophobic interaction, electrostatic interactions, and H-bonds, which may be involved in the self-assembly of SDS@ $2\beta$ -CD. In this sense, we are now attempting to access their roles one by one.

**Hydrophobic interaction.** If a solute in aqueous solution is of a hydrophobic moiety, it will enrich itself at the water–air surface and place its hydrophobic moiety towards the air to lower the surface tension. The present  $\beta$ -CD/SDS solutions exhibit water-like surface tension values ( $\sim 69$  mN m $^{-1}$ ), revealing that SDS@ $2\beta$ -CD is fully hydrophilic. Meanwhile, the local polarity in the SDS@ $2\beta$ -CD aggregates can be detected by fluorescent probes. In this case, NR was selected since it is sensitive to polarity and will be located within the aggregates. Fig. 5 lays out its emission spectra in plain water, and aqueous solutions of SDS micelles,  $\beta$ -CD, and SDS@ $2\beta$ -CD, where the latter three spectra correspond to micro-environments in micellar cores (a well-defined hydrophobic microdomain), near  $\beta$ -CD cavities, and in the SDS@ $2\beta$ -CD aggregates, respectively. Comparison of these spectra manifests that the local polarity in the SDS@ $2\beta$ -CD

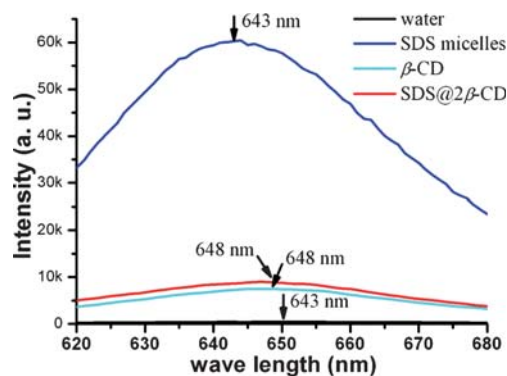


**Fig. 5** Fluorescence spectra of NR in plain water, SDS micelles (50 mM),  $\beta$ -CD aqueous solution (10 mM), and SDS@ $2\beta$ -CD solution (10 wt%).

aggregates is far more hydrophilic than that in SDS micellar cores but similar to that near  $\beta$ -CD cavities. Although  $\beta$ -CD inner cavities are hydrophobic, they cannot account for the assembly because they are isolated and covered by a polar surface. The fluorescence results, hereby, confirm the absence of a hydrophobic domain in the SDS@2 $\beta$ -CD aggregates. Moreover, thermo-gravimetric analysis (TGA) measurements of freeze-dried samples determine the water content to be  $\sim 9$  wt%, *i.e.*,  $\sim 14$  water molecules per SDS@2 $\beta$ -CD complex. The water content is likely to be contributed to by those water molecules that are present in the aggregates by forming H-bonds with  $\beta$ -CD molecules. In other words, the SDS@2 $\beta$ -CD aggregates not only have no hydrophobic domain, but also comprise a significant amount of bound water. In this case, the hydrophobic effect, therefore, can hardly contribute to the formation of SDS@2 $\beta$ -CD aggregates although it always plays a central role in traditional amphiphilic self-assembly.

**Electrostatic interaction.** Firstly, the lamellae within one tube are electrostatically stabilized, as mentioned above. Secondly, control experiments were conducted by adding salts in a large excess to screen the electrostatic interaction or substituting SDS with nonionic surfactants ( $C_{12}EO_{10}$  or  $C_{14}DMAO$ ),<sup>11</sup> both of which will result in the formation of powder precipitates. The electrostatic interaction, thus, acts as the mediator of the SDS@2 $\beta$ -CD self-assembly.

**H-bonds.** After we ruled out the possibility that the SDS@2 $\beta$ -CD self-assembly is driven by hydrophobic or electrostatic interactions, the only option is H-bonds. The following indirect experiments might support this deduction. Firstly, control experiments were performed by replacing  $\beta$ -CD with its "H-bond-poor" analogue (HP- $\beta$ -CD) to mix with SDS. In these cases, the solutions are transparent and no aggregate can be found. The control experiments suggest, to some extent, that the H-bonds between  $\beta$ -CD molecules (including the direct ones and those bridged by water) contribute to the assembly of SDS@2 $\beta$ -CD. Secondly, the presence of lateral H-bonds between CDs is possible because it was proven by single-crystal XRD for many CD complexes. For example, the H-bond network can be clearly seen for the *trans*-cinnamic acid (*tCA*)/ $\beta$ -CD complex.<sup>12</sup> Since the structure of the dimeric *tCA*/ $\beta$ -CD complex is similar to the proposed structure of SDS@2 $\beta$ -CD, the existence of lateral H-bonds between *tCA*/ $\beta$ -CD complexes suggests the possibility of lateral H-bonds between SDS@2 $\beta$ -CD complexes. In this sense, it is speculated that the SDS@2 $\beta$ -CD self-assembly is mainly driven by H-bonds.

### Ubiquitous self-assembly for CD/IS complexes

According to the proposed assembly mechanism, other CD/IS complexes are anticipated to be capable of self-assembling in water. This anticipation dose be testified for the complexes of  $\alpha$ -CD or  $\beta$ -CD with the whole class of ionic surfactants, where the studied surfactants cover anionic (SDS, SDSO<sub>3</sub>, SDBS), cationic (CTAB), and zwitterionic (TDPS) ones.<sup>11</sup> For example, these different complexes will basically form tubular structures yet with subtle differences at a CD : surfactant molar ratio of 2 : 1 and a typical total concentration of 10 wt% (Fig. 6): in the

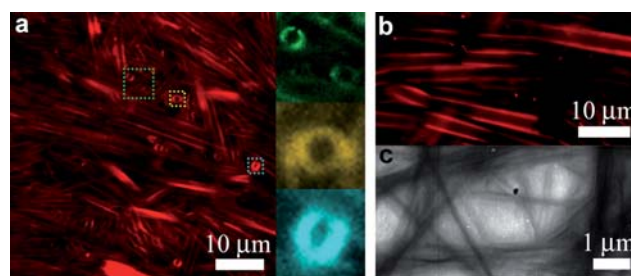


**Fig. 6** Pictures of aggregates formed by other CD/IS complexes. Microtube/vesicle coexistence for SDSO<sub>3</sub>/ $\beta$ -CD (a). Microtubes of SDBS/ $\beta$ -CD and TDPS/ $\beta$ -CD, respectively (b, c).

SDSO<sub>3</sub>/ $\beta$ -CD system, the microtubes are in equilibrium with a considerable number of giant vesicles, as highlighted by different colors (Fig. 6a); in the SDBS/ $\beta$ -CD and TDPS/ $\beta$ -CD systems, the tubes are of diameters  $\sim 3$   $\mu$ m and  $\sim 200$  nm, respectively (Fig. 6b and 6c). Straightforwardly, one can impart various properties, such as biocompatibility and stimuli-responsivity to the aggregates by simply replacing SDS with functional ionic surfactants.

### Conclusions

We have constructed a novel kind of microtube from the self-assembly of CD/IS complexes in aqueous solutions by virtue of H-bond driving and electrostatic mediation. The microtubes are characterized by a non-bundling nature, ultralong persistence lengths, highly monodispersed diameters, and remarkable stiffness, all of which may be of particular value for potential applications. The unique "annular ring" structure of the microtubes might enable the templated synthesis of multilamellar inorganic tubes in one step. Furthermore, the present hydrophilic self-assembly differs from its conventional amphiphilic counterpart in a most fundamental level, that is, the former is exclusively driven by multiple H-bonds (relatively strong and directional) but the latter relies on the hydrophobic effect (relatively weak and nondirectional). The resulting aggregates might be intrinsically more ordered and robust than the traditional ones, and the stiffness of the present microtubes gives us such a sign. In this context, this H-bond-driven hydrophilic self-assembly can complement its amphiphilic counterpart and expand the field of molecular self-assembly. In addition, the assembly behavior is general for the complexes of CDs and the entire class of ionic surfactants. It is thus envisioned that the CD/IS self-assembly systems can be readily modified or functionalized to meet broader applications by switching SDS with desired ionic surfactants. Follow-up work on how the lamellae fold into tubes and how the complexes self-assemble into bilayer structures is ongoing.

### Notes and references

- (a) G. M. Whitesides, J. P. Mathias and C. T. Seto, *Science*, 1991, **254**, 1312–1319; (b) F. M. Menger, *Proc. Natl. Acad. Sci. U. S. A.*, 2002, **99**, 4818–4821.
- For reviews, see (a) T. Shimizu, M. Masuda and H. Minamikawa, *Chem. Rev.*, 2005, **105**, 1401–1443; (b) D. T. Bong, T. D. Clark, J. R. Granja and M. R. Ghadiri, *Angew. Chem., Int. Ed.*, 2001, **40**,

- 989–1011; (c) J.-H. Fuhrhop and T. Wang, *Chem. Rev.*, 2004, **104**, 2901–2938.
- 3 (a) J. M. Schnur, *Science*, 1993, **262**, 1669–1676; (b) J. V. Selinger, M. S. Spector and J. M. Schnur, *J. Phys. Chem. B*, 2001, **105**, 7157–7169; (c) T. Shimizu, M. Kogiso and M. Masuda, *Nature*, 1996, **383**, 487–488; (d) H. Frusawa, A. Fukagawa, Y. Ikeda, J. Araki, K. Ito, G. John and T. Shimizu, *Angew. Chem., Int. Ed.*, 2003, **42**, 72–74; (e) M. Reches and E. Gazit, *Science*, 2003, **300**, 625–627; (f) M. Yemini, M. Reches, J. Rishpon and E. Gazit, *Nano Lett.*, 2005, **5**, 183–186; (g) M. Reches and E. Gazit, *Nat. Nanotechnol.*, 2006, **1**, 195–200; (h) S. Vauthey, S. Santoso, H. Gong, N. Watson and S. Zhang, *Proc. Natl. Acad. Sci. U. S. A.*, 2002, **99**, 5355–5360; (i) Y. Yamamoto, T. Fukushima, Y. Suna, N. Ishii, A. Saeki, S. Seki, S. Tagawa, M. Taniguchi, T. Kawai and T. Aida, *Science*, 2006, **314**, 1761–1764; (j) W. Zhang, W. Jin, T. Fukushima, N. Ishii and T. Aida, *Angew. Chem., Int. Ed.*, 2009, **48**, 4747–4750; (k) E. Lee, J.-K. Kim and M. Lee, *Angew. Chem., Int. Ed.*, 2009, **48**, 3657–3660.
- 4 (a) J. N. Israelachvili, *Intermolecular and Surface Forces*, Academic Press, London, 1985; (b) C. Tanford, *The Hydrophobic Effect: Formation of Micelles and Biological Membranes*, John Wiley & Sons, New York, 1973.
- 5 (a) M. R. Ghadiri, J. R. Granja, R. A. Milligan, D. E. McRee and N. Khazanovich, *Nature*, 1993, **366**, 324–327; (b) J. M. Smeenk, M. B. J. Otten, J. Thies, D. A. Tirrell, H. G. Stunnenberg and J. C. M. van Hest, *Angew. Chem., Int. Ed.*, 2005, **44**, 1968–1971.
- 6 (a) A. Harada, J. Li and M. Kamachi, *Nature*, 1992, **356**, 325–327; (b) M. V. Rekharsky and Y. Inoue, *Chem. Rev.*, 1998, **98**, 1875–1917; (c) L. X. Jiang, M. L. Deng, Y. L. Wang, Y. Yan and J. B. Huang, *J. Phys. Chem. B*, 2009, **113**, 7498–7504.
- 7 (a) A. Harada, M. Okada, J. Li and M. Kamachi, *Macromolecules*, 1995, **28**, 8406–8411; (b) V. Bernat, C. Ringard-Lefebvre, R. G. Le Bas, B. Perly, F. Djedaïni-Pilard and S. Lesieur, *Langmuir*, 2008, **24**, 3140–3149.
- 8 (a) W. M. Z. Wan Yunus, J. Taylor, D. M. Bloor, D. G. Hall and E. Wyn-Jones, *J. Phys. Chem.*, 1992, **96**, 8979–8982; (b) J. W. Park and H. J. Song, *J. Phys. Chem.*, 1989, **93**, 6454–6458.
- 9 (a) B. D. Wagner, N. S. Stojanovic, G. Leclair and C. K. Jankowski, *J. Inclusion Phenom. Macrocyclic Chem.*, 2003, **45**, 275–283; (b) P. Hazra, D. Chakrabarty, A. Chakraborty and N. Sarkar, *Chem. Phys. Lett.*, 2004, **388**, 150–157.
- 10 W. Saenger, J. Jacob, K. Gessler, T. Steiner, D. Hoffmann, H. Sanbe, K. Koizumi, S. M. Smith and T. Takaha, *Chem. Rev.*, 1998, **98**, 1787–1802.
- 11 Abbreviations: C<sub>12</sub>EO<sub>10</sub>, dodecyl *n*(ethylene oxide), *n* ≈ 10; C<sub>14</sub>DMAO, tetradecyldimethyl amine oxide; SDSO<sub>3</sub>, sodium dodecyl sulfonate; SDBS, sodium dodecyl benzene sulfonate; CTAB, cetyl trimethyl ammonium bromide; TDPS tetradecyl dimethyl ammonium propane sulfonate.
- 12 A. Kokkinou, S. Makedonopoulou and D. Mentzafos, *Carbohydr. Res.*, 2000, **328**, 135–140.